ISSN 0023-1584, Kinetics and Catalysis, 2006, Vol. 47, No. 5, pp. 686–698. © MAIK "Nauka/Interperiodica" (Russia), 2006.
Published in Russian in Kinetika i Kataliz, 2006, Vol. 47, No. 5, pp. 709–721.

Isotopic Effects on the Time-Dependences of 420 nm Ice Luminescence Excited by UV Light[1]

B. J. Selby[a], T. I. Quickenden[a†], and C. G. Freeman[b]

[a] *Chemistry, M313, School of Biomedical and Chemical Sciences, The University of Western Australia, 35 Stirling Highway, Crawley, W. A., 6009, Australia*

[b] *Department of Chemistry, University of Canterbury, Christchurch, 1, New Zealand*

**e-mail: tiq@chem.uwa.edu.au*

Received December 8, 2004

Abstract—The kinetics of the 420 nm luminescence emitted from H_2O and D_2O polycrystalline Ih ices have been studied over the 77 to 162 K temperature range. In the case of both H_2O and D_2O ices, it was found that the luminescence rise and decay curves consisted of two luminescence components, and superimposing two first-order curves with different rate constants gave the best fit to the decay and rise curves. The mean lifetimes of the two luminescence components were 1.08 ± 0.03 s and 2.47 ± 0.03 s. The rate constants were found to have negligible temperature dependences, which led to activation energies well below those obtained for either activation-limited processes or even diffusion-limited processes. Furthermore, it was found that the luminescence kinetics were not affected by isotopic substitution of D for H in the ice lattice. These observations suggest that the rate-determining step in the mechanism for the production of the luminescence is a slow (probably spin-forbidden) electronic transition that can occur at two different rates due to the presence of two different types of trapping sites in the ice lattice. A possible candidate for the electronic transition is the $^4\Sigma^- \longrightarrow X^2\Pi$ transition of excited $OH^\bullet$ radicals and not the previously suggested and ubiquitous $A^2\Sigma^+ \longrightarrow X^2\Pi$ transition of this species.

DOI: 10.1134/S0023158406050065

INTRODUCTION

Previous work from this laboratory [1–8] and by other workers [9] has established the existence of luminescence when water ice is irradiated with UV light at 260 nm, and investigations of this luminescence have been reviewed elsewhere [10]. The present paper presents some of the work from a doctoral thesis [11] produced by one of the authors (B.J. Selby).

The luminescence observed in the present study consists of two broad bands centered around 340 and 420 nm, respectively. The 340 nm luminescence contains [6] at least some emission from the Herzberg series of bands from excited molecular oxygen and decays with a lifetime that is too short to measure. Due to this short lifetime, Khusnatdov and Petrenko [9] observed only the 420 nm band.

The present paper is concerned with the time dependence of the longer lived 420 nm band. The effect of temperature and isotopic substitution on the rise and decay kinetics of the band have also been examined. The aim of these studies was to determine the mechanism for the emission of 420 nm luminescence from UV-excited ice. Previous publications from this laboratory have suggested three possible mechanisms, which are discussed below.

In addition, in some of the earlier work [8], the deposition of polycrystalline ice may not have been carried out under sufficiently stringent conditions to ensure that no amorphous ice was concurrently present. The conditions necessary to form pure polycrystalline hexagonal ice have now been reviewed (see Appendix 1) and adhered to in the present study. It is known that the morphology of the ice used does affect the luminescence decay lifetimes [7, 8].

Emitting Species

In 1992, Matich et al. reported that at least a significant portion of the 340 nm luminescence from UV-excited ice was due to excited O_2 molecules formed photolytically in the ice lattice [4, 6]. Matich also considered a number of candidate species for the longer-lived 420 nm luminescence from ice [4]. For a variety of reasons, many of these species were ruled out and only $OH^\bullet$ radicals and OH^- ions remain as possible emitters. Matich considered [4] a possible mechanism for the 420 nm emission involving excited OH^- ions, and two other mechanisms [1, 2, 7, 8] that involved excited $OH^\bullet$ radicals have been considered in other

† Deceased.

[1] This text was submitted by the authors in English.

papers from the same laboratory. The present paper presents evidence that identifies one of these mechanisms as the preferred choice.

Mechanism 1

Matich considered in [4] that the 420 nm emission from ice could be due to excited OH^- ions. Buxton et al. observed [12] an emission around 415 nm from electron-irradiated, deuterated, chloride glasses at 76 K. It was suggested by Buxton et al. that this luminescence was produced by the steps

$$e_T^- + OD \longrightarrow OD^-{}^*, \quad \text{(I)}$$

$$OD^-{}^* \longrightarrow OD^- + h\nu\ (415\ \text{nm}). \quad \text{(II)}$$

It has been pointed out [4] that this mechanism in UV-excited ice was energetically viable. However, it has also been pointed out [4] that the rate of formation of excited OD^- ions would be regulated by the diffusion of $OD^\cdot$ radicals to the trapped electrons, e_T^-. Matich calculated [4], for the above mechanism, that the ratio of the rate constants for H_2O and D_2O ice (k_{OH}/k_{OD}) would be 1.03 and would be too close to unity to distinguish with the present equipment. However, this calculation was based on diffusion in the gas phase and is not applicable to the solid state, where diffusion occurs very differently. Later, in the present paper, we point out that if this mechanism is responsible for the 420 nm emission from UV-excited ice, then an expected isotopic ratio of around 1.27 is more likely. Such a ratio would be easily detectable in the present study.

In addition, if the above mechanism is correct, then the luminescence rise and decay curves would be well fitted by a second-order or, perhaps, pseudo-first-order kinetic model. Furthermore, the activation energy obtained from such fits would have to be consistent with that for the diffusion of $OH^\cdot$ radicals.

Mechanism 2

The $A^2\Sigma \longrightarrow X^2\Pi$ transition of $OH^\cdot$ is ubiquitous in the gas phase and tends to dominate all the spectra of gas phase systems that are either electrically or optically excited at low pressure unless the gases have been very carefully dried. Hence, it was not surprising that, in the early work by this laboratory, Litjens suggested [1, 2] that the 420 nm luminescence from UV-excited ice was due to the following series of steps, which lead to the $A^2\Sigma \longrightarrow X^2\Pi$ transition of $OH^\cdot$ radicals:

$$H_2O \xrightarrow{h\nu_1} OH^\cdot + H, \quad \text{(III)}$$

$$OH^\cdot + OH^\cdot \longrightarrow H_2O_2, \quad \text{(IV)}$$

$$H_2O_2 \xrightarrow{h\nu_1} OH^* + OH^\cdot + L, \quad \text{(V)}$$

$$OH^* + L \longrightarrow OH_L^*, \quad \text{(VI)}$$

$$OH_L^* \longrightarrow OH_L^\cdot + h\nu_2. \quad \text{(VII)}$$

Here, the rate-determining step is process (IV) and the symbol L represents an ice lattice vacancy. The excited state of $OH^\cdot$ (OH^*) is $A^2\Sigma^+$, and $h\nu_1$ refers to the 260 nm exciting radiation, while $h\nu_2$ refers to the 420 nm luminescence. If the above mechanism is correct, then a second-order or pseudo-first-order time dependence of the luminescence rise and decay curves would be expected. Furthermore, the activation energy would have to be consistent with that expected for the diffusion-limited process:

$$OH^* + L \longrightarrow OH_L^*.$$

It is also pointed out later in the present paper that if the above mechanism is correct and the above process is the rate-determining step, then a kinetic isotopic ratio (k_{OH}/k_{OD}) of 1.27 would be expected.

Mechanism 3

The double first-order model is based on the idea that the rate-determining step is a slow, possibly spin-forbidden, electronic transition. Hence, the mechanism suggested by Quickenden et al. [7, 8] is a likely possibility. This mechanism is as follows:

The first step is the fast photodissociation of H_2O (or D_2O in the present work) into the ground state $OH^\cdot$ (or $OD^\cdot$) and H (or D) according to the following:

$$H_2O + h\nu\ (260\ \text{nm}) \xrightarrow{\text{fast}} OH^\cdot\,(X^2\Pi) + H. \quad \text{(VIII)}$$

Although some researchers may express surprise that significant optical absorption may occur in ice at wavelengths in the 200–300 nm region, there is strong evidence that this does indeed occur in a detectable manner in liquid water. This matter is discussed further in the Choice of Mechanism section of the Results and Discussion.

At least some of the $OH^\cdot$ radicals produced then fall into traps, T, within the ice lattice. This step is also fast:

$$OH^\cdot\,(X^2\Pi) + T \xrightarrow{\text{fast}} OH_T^\cdot\,(X^2\Pi). \quad \text{(IX)}$$

It is believed that, at temperatures below about 100 K, the $OH^\cdot$ radicals are stable in these traps but that, at higher temperatures, they become mobile. This explains the lower luminescence intensities observed at higher temperatures. The trapped $OH^\cdot$ radicals are then excited to their $A^2\Sigma^+$ state and then, via intersystem crossing, to their $^4\Sigma^-$ state (Fig. 1) according to the following:

$$OH_T^\cdot(X^2\Pi) + h\nu\ (260\ \text{nm}) \xrightarrow{\text{fast}} OH_T^*(A^2\Sigma^+) \xrightarrow{\text{fast}} OH_T^*(^4\Sigma^-). \quad \text{(X)}$$

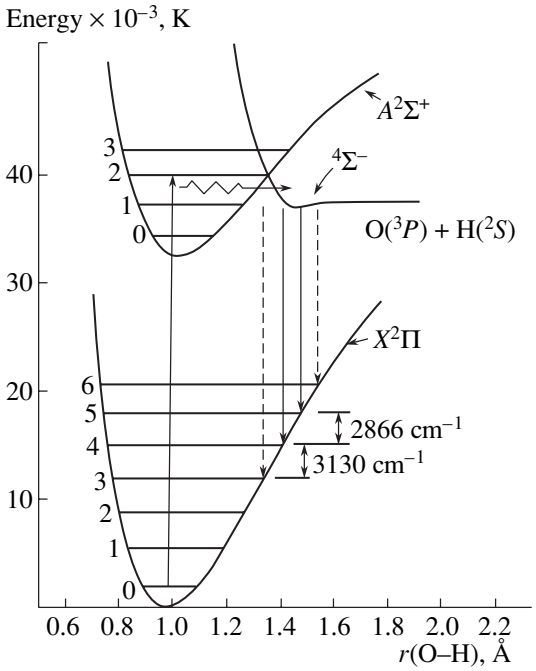

Fig. 1. The proposed transition responsible for the 420 nm luminescence from UV-excited ice.

Again, these are fast processes.

It is then proposed that the excited OH* radicals decay back to their ground state via the following:

$$OH_T^* (^4\Sigma^-) \longrightarrow OH_T^{\cdot} (X^2\Pi) + h\nu\ (420\ \text{nm}). \qquad \text{(XI)}$$

This transition is spin forbidden and, as a result, would occur somewhat slowly (over several seconds). It would be the rate-determining step accounting for the observed lifetime of the luminescence rise and decay.

It has been tentatively suggested in the past [7, 8] that there are two different kinds of traps present in the ice lattice. This would result in double-first-order kinetics. Hence, if the above mechanism is correct, then first-order (or, more correctly, double-first-order) time dependences would be observed. Furthermore, negligible activation energies would be observed, and there would be no detectable isotopic effects on the rise and decay of the 420 nm luminescence.

The principal difficulty with this proposed mechanism is that the quartet state of $OH^{\cdot}$ is dissociative in the gas phase. However, perturbations in the ice matrix could make it associative [7, 13]. A diagram of the quartet state and the proposed transition is shown in Fig. 1.

EXPERIMENTAL

The ice samples used in this study were made under conditions that are known (see Appendix 1) to produce polycrystalline ice Ih by the vacuum deposition of water vapor onto a copper substrate at 200 ± 1 K (1). The equipment and procedures used to make the H_2O ice and measure its luminescence have been fully described in previous publications [4, 6–8] and involve using a high vacuum chamber maintained at a pressure of ca. ~10^{-5} Torr by a turbomolecular pump system (Leybold Heraeus Turbovac 150).

The vacuum chamber contained an ice sample mounted on a copper block that was refrigerated by a flow of liquid nitrogen from a gravity feed tank. The ice was irradiated with doubly monochromated UV light from a water-cooled xenon lamp system (Photon Technology Int., LPS 200X). Monochromated luminescence was detected with an EMI 9813 QA photomultiplier tube, which is sensitive in the 200–600 nm wavelength range. The tube was operated in the photon-counting mode. All the bandpasses were set to 20 nm throughout the present work.

Several improvements were made to the deposition system prior to beginning the present investigation. Firstly, the rate of deposition was more carefully controlled by using a stop valve in series with the variable leak valve used to control the deposition rate. This enabled the variable leak valve to be set to a fixed value and left unchanged, which reduced the significant variations in the flow rate that occur when the leak valve is closed and reopened. The second improvement to the deposition system was the addition of a thermostat bath around the vessel containing the H_2O or D_2O that was being deposited. This further improved the reproducibility of the deposition rate. The flow rate used in this study was $(2.2 \pm 0.1) \times 10^{22}$ molecules/h, and the samples were deposited for a period of 40 min.

After deposition, the ice samples were cooled to 78 K and then left (without irradiation) for a period of two hours for the luminescence intensity to stabilize. This stabilization period is necessary because it has been shown [8] that the luminescence intensity grows slowly over this time before reaching a more steady value.

Similar equipment and procedures were used to make the D_2O ice and to measure its UV excited emissions. However additional steps were taken to ensure that the isotopic purity of the D_2O was maintained. As in the case of the H_2O, in order to ensure the absence of potentially luminescent chemical impurities in the D_2O, the latter was distilled in a double stage still. This still was similar to that used in [4] to prepare triply distilled H_2O from singly distilled H_2O, with the first stage being an oxidative one as for the H_2O. After distillation, the isotopic purity of the D_2O was found (using an NMR technique) to be (97.0 ± 0.4)%. In this technique, the amount of protium impurity in the D_2O was determined from the area under the protium NMR line.

In order to measure the luminescence rise curve, a shutter on the exciting UV light source was suddenly opened so that the ice samples were exposed to 260 nm radiation. The opening of the shutter took place in a time of ca. 0.03 s. The resulting rise in the intensity of

the 420 nm luminescence band was then measured. For observation of the decay curve, the shutter was suddenly closed and the resulting fall in the luminescence intensity was recorded. In this case, the shuttering took place in a time of ca. 0.09 s. To remove any effect of the shuttering process from the luminescence rise and decay curves, the data obtained in the first 0.3 s was removed from each curve prior to fitting the kinetic expressions.

Ice luminescence experiments were performed in an evacuated chamber at a gas pressure of ca. ~10^{-5} Torr. Experiments were performed to test the possibility that the luminescence might have arisen from traces of air or O_2 that had either been left in the ice during the deposition or that subsequently entered the ice from the imperfect vacuum. These experiments involved deliberately saturating the water with air prior to the deposition of the ice and then examining the effect of this procedure on the ice luminescence. No significant effects on the luminescence intensity or kinetics were detected. It is thus clear that the air neither contributes to nor affects the observed luminescence.

RESULTS AND DISCUSSION

Fitting the Time Dependence of the Luminescence with Various Kinetic Models

Luminescence rise and decay results were obtained for eight samples of polycrystalline H_2O ice and eight samples of polycrystalline D_2O ice. For each sample, measurements were taken at six different temperatures. At each of these six temperatures, a set of five replicate rise and five replicate decay curves were recorded. By averaging the five decay curves in each set, a mean decay curve was obtained for each of the six temperatures considered for each sample.[1] The rise data was treated in a similar way whence a mean rise curve was also obtained at each of the six temperatures for each ice sample.

The above mean rise and decay curves were then fitted to the following eight kinetic models, which have been presented elsewhere [14]. These were the following:

I—A double-first-order model,

II—A fractal pseudo-first-order model,

III—A fractal second-order model with unequal concentrations,

IV—A second-order model with unequal concentrations,

V—A simple first-order model,

VI—A fractal second-order model with equal concentrations,

VII—A second-order model with equal concentrations, and

VIII—A tunneling model.

As a large number of fits were carried out, graphical presentations for all the fits are not provided. However, Fig. 2 shows the model giving the best fit for the decay data and the model giving the worst fit to the decay in the case of one typical ice sample.

Figure 3 shows a typical rise of the luminescence data to a plateau value. Decay data were obtained by shuttering the exciting light after the plateau value was reached to give decays of the type shown in Fig. 2.

A kinetic model was considered to fit the experimental data well if it satisfied several criteria. First, such a model produced a low value for the square root of the sum of the squared residuals (SqSSR) when fitted to both the rise and decay curves.[2] The second criterion is the correlation of the residuals, which are defined as the differences between the experimentally measured luminescence intensities and those predicted by the fitted equation at each point on the decay or rise curve. If a model fits the data well, the differences between the measured and predicted intensities should be completely random, which means that the residuals should not show correlation.

A kinetic model that fits both the rise and decay luminescence data with low SqSSR values and uncorrelated residuals must also be considered against three other criteria. Firstly, and of prime importance, the parameters obtained from the rise fits must show good agreement with those obtained from the decay fits. Sec-

[1] It should he noted that the treatment of the data in the present work differs somewhat from the method used in previous work [8]. In that earlier work, replicate decay data for different samples were averaged before the curve lifting was carried out. This was not done in the present work. Instead, each individual set of decay or rise data was separately fitted to the integrated rate equation for a kinetic model and the fitting parameters from the replicate fits were then averaged. Although the method used in the present work is a lot more time consuming (it required 576 fits for separate sets of decay data alone and further fits to the rise data), it had the following advantages. Firstly, it enabled a set of fitting parameters to be derived from each sample so that, with a number of samples, the variation in these parameters is easily assessed, and a reliable 95% confidence interval could thus be found for each parameter. If the aggregated data method in [8] is used, this cannot be done as only one fit from each temperature is performed and the variation between runs may be hidden. Secondly, it has been shown [14] that averaging decay curves from different samples is incorrect when considering second-order models because the normalization process is then invalid. Hence, to consider second-order models rigorously, one must resort to fitting the results from each ice sample individually.

[2] In this work, the square root of the sum of the squared residuals is used to examine the quality of the curve lining. Previous works [2, 4, 7, 8] have often used the sum of the squared residuals for this purpose. However, it is often considered more convenient to take the square root of this number. This has been done in the present work for two reasons: (1) the fitting program used automatically takes the square root and (2) taking the square root preserves the units of the quantity being fitted. Whether the SqSSR value or the SSR value is used, the final choice of the model will be unchanged since this choice depends only on which model has the minimum SqSSR or SSR value. If the SqSSR value is a minimum, then the SSR value will also be a minimum and vice versa because the square root function and the square function are strictly increasing functions for a domain rather than zero.

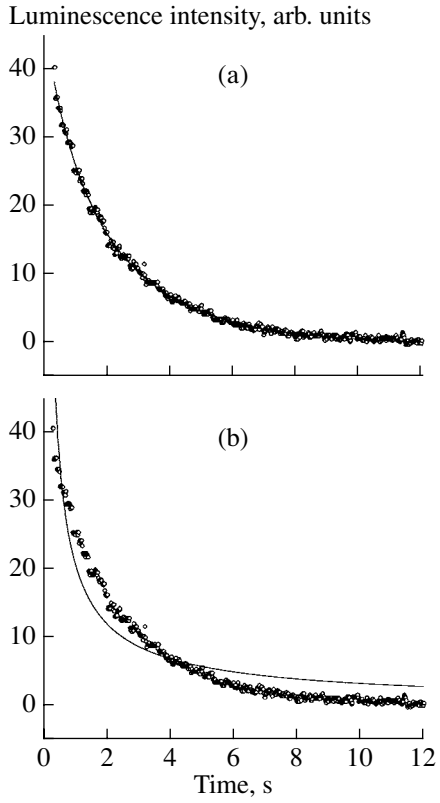

Fig. 2. Fits of the double first-order model (top) and the tunneling model (bottom) to the 420 nm luminescence decay curve from one H_2O ice sample at 78 K. The circles represent the experimentally measured luminescence intensities, and the solid curves are the fitted functions.

ondly, the activation energy predicted by the model for the rate-determining step in the production of the luminescence must match that observed experimentally. Finally, the experimentally observed effect of isotopic substitution on the kinetics must be correctly predicted by the model.

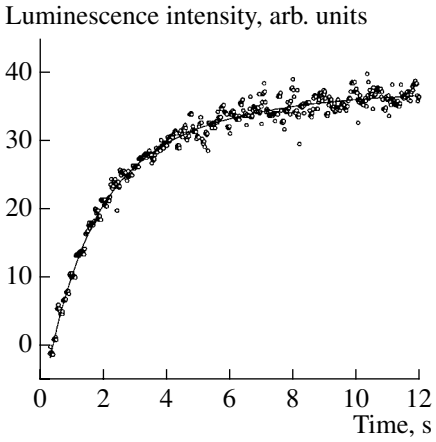

Fig. 3. Fit of the double first-order model to the 420 nm luminescence rise curve from one H_2O ice sample at 78 K. The circles represent the experimentally measured luminescence intensities, and the solid curve is the fitted function.

The relative merits of the different proposed models are presented in Table 1.

It is clear that the best fit to the time dependent intensity data is given by the double-first-order model as it meets all the criteria for the goodness of fit in Table 1.

In the case of the double-first-order model, the luminescence consists of two components, one short-lived and the other long-lived. The total luminescence intensity rises according to [14]

$$L = a(1 - \exp(-k_a t)) + b(1 - \exp(-k_b t)) + c \quad (1)$$

and decays according to [14]

$$L = a\exp(-k_a t) + b\exp(-k_b t). \quad (2)$$

Here, L is the luminescence intensity at the time t; k_a and k_b are the first-order rate constants for the short-lived and long-lived component of the luminescence,

Table 1. The kinetic models fitted to the rise and decay of the 420 nm luminescence from UV-excited H_2O and D_2O ices

	Model no.							
	I	II	III	IV	V	VI	VII	VIII
Short model nam	Yes	Yes	Yes	Yes	No	No for D_2O, Yes for H_2O	No for D_2O, Yes for H_2O	No
Low SqSSR for decay fits	Yes	Yes	Yes	Yes	No	No	No	No
Uncorrelated residuals for decay fits	Yes	Yes, but biased*	Yes	Yes, but**	No	NT***	NT	NT
Low SqSSR for rise fit	Yes	Yes	Yes	No	No	NT	NT	NT
Uncorrelated residuals for rise fits	Yes	No	No	Yes	NT	NT	NT	NT
Correctly predicted E_a	Yes	NT	NT	Yes	Yes	NT	No	NT
Correctly predicted isotopic effects	Yes	NT	NT	No	Yes	NT	No	NT

* The extra steps involved in the numerical differentiation and smoothing the data will cause a lower SqSSR.

** The fitting program frequently produced errors, and, furthermore, the errors in the parameters were larger than the parameters themselves.

*** "NT" indicates untested.

Table 2. Ice luminescences at 420 nm from H_2O ice. Lifetimes obtained by fitting the double first-order model. Each entry in the table is the weighted mean of eight replicate fits performed on the time-dependent luminescence from eight different H_2O ice samples. The errors shown are 95% c.i.'s in these means

Temp., K	Short-lived luminescence component		Long-lived luminescence component	
	decay lifetime/s	rise lifetime/s	decay lifetime/s	rise lifetime/s
78	1.220 ± 0.160	1.270 ± 0.110	2.554 ± 0.027	2.45 ± 0.10
99	0.888 ± 0.067	0.991 ± 0.066	2.403 ± 0.046	2.364 ± 0.067
117	1.072 ± 0.094	1.39 ± 0.12	2.532 ± 0.049	2.160 ± 0.065
132	0.913 ± 0.072	1.200 ± 0.065	2.283 ± 0.068	2.85 ± 0.12
147	1.041 ± 0.086	1.295 ± 0.077	2.20 ± 0.15	2.17 ± 0.18
162	1.160 ± 0.098	0.97 ± 0.12	3.320 ± 0.290	2.47 ± 0.29

Table 3. Ice luminescences at 420 nm from D_2O ice. Lifetimes obtained by fitting the double first-order model. Each entry in the table is the weighted mean of eight replicate fits performed on the time-dependent luminescence from eight different D_2O ice samples. The errors shown are 95% c.i.'s in these means

Temp., K	Short-lived luminescence component		Long-lived luminescence component	
	decay lifetime/s	rise lifetime/s	decay lifetime/s	rise lifetime/s
78	1.12 ± 0.14	1.20 ± 0.19	2.545 ± 0.065	2.340 ± 0.041
99	1.164 ± 0.089	1.06 ± 0.12	2.632 ± 0.083	2.60 ± 0.12
117	0.892 ± 0.017	0.93 ± 0.10	2.731 ± 0.060	2.273 ± 0.057
132	1.209 ± 0.079	1.178 ± 0.097	2.66 ± 0.11	2.27 ± 0.11
147	1.399 ± 0.094	1.32 ± 0.11	2.18 ± 0.17	2.48 ± 0.17
162	0.79 ± 0.14	0.855 ± 0.080	2.2 ± 1.2	2.15 ± 0.18

respectively; the parameters a and b give the relative contributions of the short-lived and long-lived components of the luminescence, respectively; and c is a constant. The role of this constant has been discussed elsewhere [14].

The fitting of the preferred double-first-order model gives the fitted rate constants (and lifetimes) for both the H_2O and D_2O ice isotopomers shown in Tables 2 and 3. It should be noted that the mean luminescence lifetimes are, as usual, defined as the inverse of the relevant rate constants.

The acceptance of the double-first-order model as the correct one to describe the kinetics of the 420 nm ice luminescence implies that the rate-determining step for the production of this luminescence is a slow electronic transition rather than an activation-limited or diffusion-limited process. This is consistent with mechanism No. 3 in the Introduction but not mechanisms 1 or 2.

Temperature Dependences of the Luminescence Lifetimes

The mean lifetimes are the inverses of the corresponding luminescence decay rate constants and are given below in seconds in Tables 2 and 3.

It was observed that, for each ice sample, the initial luminescence intensities (and the subsequent intensities) all fell off sharply with increasing temperature. However, most importantly, the mean lifetime did not show significant variation with temperature, and this led to the very low (virtually negligible) activation energies discussed below.

Arrhenius plots may be constructed for each column of lifetime data in Tables 2 and 3. When this is done, the activation energies so determined for the rate-determining steps in the production of the 420 nm luminescence will be found to be negligible.

As the rise and fall data for the double-first-order model show good consistency (see Tables 2, 3) and there is little evidence for isotopic shifts (see below), it was considered acceptable to average the activation energies across both isotopomers and the rise and fall data. This enabled one to obtain upper limits for the very small activation energies for both the long-lived and short-lived components of the luminescence. These limits are displayed in Table 4, along with literature values for various low activation energies associated with processes in ice.

Table 4 shows that the activation energies determined in the present study are very much lower than any of the published values reported for the chemical

Table 4. A comparison of the activation energies determined in the present study with published values for various processes that could occur in ice

Species	Process	E_a, eV	Temp., K	Authors
H	Decay	ca. 0.043–0.110	30–50	Flournoy et al. [15]
H	Decay	ca. 0.40*	77–87	Plonka et al. [16]
H^+	Mobility	0.021	96–106	Eckener et al. [17]
H^+	Mobility	0.041	108–118	Eckener et al. [17]
e^-	Decay measured by conductivity measurements	0.1–0.2	77–130	Warman et al. [18]
$OH^\bullet$	Decay	0.26 ± 0.02	92–107	Siegel et al. [19]
$OH^\bullet$	Decay measured by luminescence measurements	0.017	77–200	Maria and McGlynn [13]
Luminescence decay (fast) upper limit		4.1×10^{-5}	78–162	Present study
Luminescence decay (slow) upper limit		7.2×10^{-4}	78–162	Present study

* Using the time independent part of the time-dependent second-order (fractal) rate coefficient.

Table 5. Rate constant ratios for the 420 nm luminescence from the H_2O and D_2O ices averaged across all the temperatures

Rise or fall	Luminescence component	Mean k_H/k_D across all temperatures with 95% c.i.'s	Maximum possible isotopic shift
Fall	Short-lived	1.0 ± 0.1	10%
Fall	Long-lived	1.05 ± 0.03	3%
Rise	Short-lived	0.91 ± 0.07	7%
Rise	Long-lived	0.98 ± 0.05	5%

processes that might occur in the ice lattice. The activation energies obtained in the present study most closely match the activation energy observed by Maria and McGlynn [13] for the decay of $OH^\bullet$ radicals measured by luminescence decay kinetics. This result is very significant as it is proposed that the luminescence observed in the present study from pure ices arises from the same transition as that observed by those authors for alkaline ices. Nevertheless, the activation energies determined in the present study are still several orders of magnitude lower than those reported by Maria and McGlynn [13]. Their values might be expected to differ as amorphous ice samples were used, and these are likely to have been annealed irreversibly as the temperature was raised to obtain the Arrhenius plots. Such annealing could have altered the values of the rate constants and the derived activation energies. Furthermore, it must also be noted that Maria and McGlynn used [13] ice doped with hydroxide ions rather than the pure ice used in the present work.

Examination of the data in Table 4 makes it quite clear that the activation energies obtained in the present study are negligible and indicates that the rate-determining step for the 420 nm luminescence is clearly not an activation limited process. These activation energies are even too small to be explained by diffusion-limited kinetics. Thus, it must be concluded that the rate-determining processes involved in the production of the 420 nm luminescence are most probably simply the decays of excited species. This is consistent with mechanism 3 in the Introduction, but not mechanisms 1 or 2, and is further evidence in favor of mechanism 3.

Isotopic Effects on the Luminescence Lifetimes

Because of the larger error bars attached to the k_H/k_D values determined at individual temperatures and the lack of an effect of temperature on the rate constants, it was decided to average the results across all the temperatures used. This procedure is justified by the negligible effect of temperature on the rate constants, which of course reflects the very low activation energies. The results of averaging the k_H/k_D ratio across temperatures are shown in Table 5, which also shows the maximum possible isotopic shift.

The predicted isotopic shifts for various mechanisms that could be responsible for the 420 nm luminescence from ice are now considered.

Diffusion of $OH^\bullet$ or $OD^\bullet$ radicals in ice. Consider mechanism 1 and 2 from the Introduction. If either of these mechanisms were correct, then the rate-limiting step would be the diffusion of $OH^\bullet$ radicals through the ice. Hence, the rate constant would be directly proportional to the diffusion coefficient, D_A, of the $OH^\bullet$ (or $OD^\bullet$) radicals.

At present, reliable values of D_A for the diffusion of $OH^{\bullet}$ and $OD^{\bullet}$ in water ice are not available, presumably because of measurement difficulties [20, 21]. However, Crowell and Bartels [22] have calculated values for the diffusion coefficients of $OH^{\bullet}$ and $OD^{\bullet}$ in the *liquid phase*, and, using these values, an isotopic ratio (k_H/k_D) of 1.27 would be expected for the mechanism of the ice luminescence proposed by Litjens [1, 2]. A similar ratio is obtained using the liquid phase data in [23].

Although it is not ideal, the use of liquid phase values for the diffusion coefficient of $OH^{\bullet}$ radicals in ice can be justified by reference to the work by Taub and Eiben [24] and Ghormley and Hochanadel [25]. These researchers have reported that the diffusion coefficient for mobile (untrapped) $OH^{\bullet}$ radicals in ice is approximately the same as for $OH^{\bullet}$ radicals in liquid water. Unfortunately, the above authors did not examine the diffusion of $OD^{\bullet}$ in D_2O ice.

The effect on lifetimes of excited states. The rate determining step in mechanism 3 in the Introduction is a slow electronic transition. The effect of isotopic substitution on the lifetime of an excited species is negligible (see Appendix 2). If mechanism 3 is the correct mechanism for the 420 nm luminescence, then substitution of the isotopic wavelength shift into the Einstein coefficient for spontaneous emission gives an expected change in the lifetime of ca. 1.0% when D_2O ice is substituted for H_2O ice. Such a small change would be undetectable in the present work.

Comparison between the above predicted isotopic effects and the experimentally observed effects in the present study. Table 6 compares the above predicted isotopic effects with the isotopic effects on the kinetics that were observed in the present study. Table 6 gives the maximum possible shift in the case of both the short-lived and long-lived luminescence components. In each case, two possible values (for the rise and fall) are available (see Table 5). However, since the *maximum* possible shift is being considered here, the larger of the two values was used in each case.

Consider mechanism 1 and 2 in the Introduction. If either of these mechanisms were responsible for the 420 nm luminescence, an isotopic ratio (k_H/k_D) of 1.27 would be expected as indicated above. Quite clearly, the experimentally determined values of k_H/k_D in Table 5 show that the production of ice luminescence is not controlled by the diffusion-limited migration of $OH^{\bullet}$ (or $OD^{\bullet}$) through the ice lattice. This provides further evidence against mechanisms 1 and 2. Furthermore, any other mechanisms in which the rate-determining step is the diffusion of $OH^{\bullet}$ (or $OD^{\bullet}$) are also ruled out.

Table 6. Predicted isotopic shifts at 78 K for the various reaction mechanisms that might be responsible for the 420 nm emission from UV-excited ice

Rate-determining step in the mechanism	Predicted isotopic shift, k_H/k_D	Predicted isotopic shift
Excited $OH^{\bullet}$ (or $OD^{\bullet}$) decay	0.99	1%
$OH^{\bullet}$ (or $OD^{\bullet}$) diffusion	1.27	27%
Maximum possible shift in the present work (short-lived)	1.00 ± 0.10	10%
Maximum possible shift in the present work (long-lived)	0.98 ± 0.05	5%

The lack of an isotopic effect on the reaction rate in the present work is inconsistent with the rate-determining step being an activation-limited or diffusion-limited process, but it is consistent with the rate-determining step being an electronic transition, as in mechanism 3 in the Introduction. This is further evidence in support of this mechanism.

The Choice of Mechanism for the 420 nm Luminescence from UV-Excited Ice

Out of the three possible mechanisms considered in the Introduction, neither mechanism 1 nor 2 are consistent with the observations mentioned above, and, accordingly, they must be rejected. Mechanism 3, however, is consistent with all of the above observations, and, therefore, this mechanism, which was originally proposed for the luminescence from alkaline ices by Maria and McGlynn [13], is proposed for the 420 nm emission from UV-excited ice.

The main difficulty with the proposed mechanism is that the quartet state of $OH^{\bullet}$ is dissociative in the gas phase. However, it is quite possible [7, 13] that the perturbations from the ice matrix make the quartet state associative in the solid state.

A second objection may arise because of the common belief that H_2O ice and water are completely transparent in the 200–300 nm region of the spectrum; hence, the excitation step (Eq. (VIII)) by ultraviolet light would not be possible. Whilst this view is partly correct, particularly as one approaches 400 nm, there is still a residual absorption of ultraviolet light from the tail of the $\tilde{X}\,^1A_1 \longrightarrow {}^1B_1$ absorption band of the H_2O molecule (centered around 160 nm) in the vacuum UV. This leads to the UV absorption tail of liquid water, about which we previously published [26], and still shows detectable absorption even out as far as 300 nm [27].

It has been tentatively proposed by others [7, 8] that there are two different kinds of traps present[3] in the ice lattice, and this would account for the observed double-first-order kinetic behavior. In the past, it has been assumed that the two decays from the different lattice sites must occur independently, but, as is discussed elsewhere [14], it is possible that the two decays could be coupled according to the following:

$$\begin{array}{ccc} OH^{\cdot}_{T_1} + h\nu_{1,2} & \overset{\text{fast}}{\rightleftharpoons} & OH^{*}_{T_1} \\ + & & + \\ T_2 & & T_2 \\ \updownarrow & & \updownarrow \\ OH^{\cdot}_{T_2} + h\nu_{1,2} & \overset{\text{fast}}{\rightleftharpoons} & OH^{*}_{T_2} \\ + & & + \\ T_1 & & T_1 \end{array} \qquad \text{(XII)}$$

Here, T_1 and T_2 represent the two types of traps, and $h\nu_1$ represents the exciting radiation and $h\nu_2$ represents the emitted light. However, this coupled proposal seems unlikely if the species are trapped, as they would have to be mobile to move between traps. Hence, the original uncoupled option is more likely.

Another possible alternative version of the quartet mechanism is one in which excited OH* is formed in both trapped and untrapped environments:

$$\begin{array}{ccc} OH^{\cdot}_{T} + h\nu & \overset{\text{fast}}{\underset{k_A}{\rightleftharpoons}} & OH^{*}_{T} \\ k'_{BA}\uparrow\downarrow k'_{AB} & & k'_{BA}\uparrow\downarrow k'_{AB} \\ OH^{\cdot} + h\nu & \overset{\text{fast}}{\underset{k_B}{\rightleftharpoons}} & OH^{*} \\ + & & + \\ T & & T \end{array} \qquad \text{(XIII)}$$

This alternative is considered unlikely for two reasons. Firstly, a significant wavelength shift would be expected between emissions arising from the trapped and untrapped $OH^{\cdot}$ radicals. Previous experimental studies [6] have ruled out such a wavelength shift. Furthermore, it is expected that the untrapped $OH^{\cdot}$ would be very quickly destroyed by scavenger molecules. Hence this alternative is considered unlikely.

It is rather interesting that the ubiquitous $A^2\Sigma^+ \longrightarrow X^2\Pi$ transition of $OH^{\cdot}$ radicals appears, at first sight, to be absent from the emission spectrum of UV-excited ice. The $A^2\Sigma^+ \longrightarrow X^2\Pi$ transition is much too short-lived to be consistent with the lifetimes observed in the present study. Therefore, if this transition was responsible for the 420 nm emission, it could only be explained by invoking a series of steps, such as mechanism 2, in which a diffusion-limited or activation-limited precursor process is the rate-determining step. However, it is clearly shown in the present paper that a diffusion-limited or activation-limited precursor process cannot be the rate-determining step.

Although the $A^2\Sigma^+ \longrightarrow X^2\Pi$ transition of $OH^{\cdot}$ radicals cannot be the cause of the long-lived emission around 420 nm observed in the present study, it is possible that such a transition is still responsible for a minor component of the 420 nm emission from UV-excited ice. Such a component would be short-lived and superimposed on the longer lived component observed in the present study. If this were indeed the case, the short-lived component of the luminescence due to the $A^2\Sigma^+ \longrightarrow X^2\Pi$ transition of $OH^{\cdot}$ (or $OD^{\cdot}$) radicals would have been lost when the initial data was truncated from the decay and rise curves.

CONCLUSIONS

The kinetics of the 420 nm luminescence from UV-excited H_2O and D_2O ice have been examined. It was concluded that the rate-determining step in the production of the luminescence is neither a diffusion controlled nor an activation controlled process but is a slow electronic transition. This transition is most likely to be the $^4\Sigma^- \longrightarrow X^2\Pi$ transition of $OH^{\cdot}$ (or $OD^{\cdot}$) radicals formed photolytically in the ice.

APPENDIX 1

REVIEW OF ICE MORPHOLOGY

This appendix will review the formation of hexagonal polycrystalline ice (Ih) from water vapor. Ice exists in a number of different morphologies [28]. One such form of ice that has been given particular attention is ice I. This has a cubic modification known as ice Ic and a hexagonal modification known as ice Ih. Ice also exists in a disordered form known variously as amorphous ice, vitreous ice, and amorphous solid water.

Previous Methods Used by the Present Research Group for Making Polycrystalline Ice

In early work by the present research group, Freeman et al. [29] attempted to make hexagonal polycrystalline ice (Ih) in two ways. One way was by annealing amorphous ice samples at 204 K. This method would probably produce polycrystalline Ih, but it is difficult to be certain that the entire sample has been annealed. (See the discussion on this technique later in this appendix.) The other method used by Freeman et al. [29] was depositing water vapor at 97 K at rates that were 500 to 2500 times greater than those rates used for amorphous ice. Later, work by the present research group [8] used a similar procedure where ice samples were deposited at 78 K at rates ca. 300 times faster than the maximum

[3] There is strong EPR evidence [54, 55] that shows that there are more than one type of trapped $OH^{\cdot}$ in crystalline ice. It is clear from that work that there are three different orientations which the $OH^{\cdot}$ radical can adopt and that these differ primarily in their hydrogen bonding. The question of why only two different types of OH sites appear in emission work will need to be resolved in a future study.

allowable rate for forming amorphous ice. However, in the light of a recent and more detailed review of the literature, it was found that ice deposited under such conditions may possibly be a mixture of both cubic polycrystalline ice (Ic) and amorphous ice.

In order to justify that their ice was indeed hexagonal polycrystalline ice, the above researchers [8, 29] refer to Sivakumar et al. [30]. However Sivakumar et al. [30] did not make polycrystalline ice by depositing vapor at a high flow rate. Rather, they claim that they made both polycrystalline ice Ih and amorphous ice by using the same flow rate but at a temperature below 110 K to deposit the amorphous ice and a temperature of 150 K to deposit the polycrystalline ice. Sivakumar et al. [30] give a flow rate maximum for forming amorphous ice at temperatures below 110 K, but they do not actually say which sort of ice morphology is obtained if this flow rate is exceeded. In addition, the morphologies of the samples used by Sivakumar et al. [30] are not all that clear because the samples were studied by Raman spectroscopy and no definitive structural methods such as X-ray diffraction were used.

A thorough literature search has now been conducted in order to clarify the conditions for producing the various morphologies of ice. During this search, it was found that Narten et al. [31] deposited ice at 77 K with almost the same flow rate (ca. 300 mg/h) as used by the Quickenden Research Group in [7]. Narten et al. [31] used X-ray diffraction to show that the sample was not polycrystalline ice Ih but was, in fact, cubic polycrystalline ice Ic mixed with amorphous ice. When this sample was heated to 150 K, it was found that it rapidly and completely converted to hexagonal polycrystalline ice Ih. Upon cooling back to 77 K, the sample retained the Ih morphology. In light of this evidence, it is quite possible that the ice samples studied by the present research group in the past have actually been mixtures of amorphous ice and cubic polycrystalline ice, rather than pure hexagonal polycrystalline ice as claimed.

Production of Polycrystalline Ice by Annealing Amorphous Ice

A number of reports [31–38] have been made in the literature about amorphous ice deposited at low temperatures being heated to become polycrystalline ice Ic and, then, the ice Ic becoming polycrystalline ice Ih on further heating. Hobbs [28] summarizes much of the work in this area. Although there is little doubt that amorphous ice transforms to polycrystalline ice Ic upon heating and to polycrystalline ice Ih upon further heating, there is poor agreement upon the exact temperatures where these changes take place [34]. There is also wide disagreement on how rapidly and completely the changes occur. Hobbs points out in his major review [28] that, although ice Ic transforms irreversibly to ice Ih above 173 K, it tends to do so rather sluggishly and, furthermore, the rate of conversion is dependent on the thermal history of the sample. Hence, the disagreement in the literature, which will now be discussed.

As mentioned above, Narten et al. [31] claim that ice deposited from vapor at about 300 mg/h and a substrate temperature of 77 K is a mixture of amorphous and polycrystalline ice Ic and that rapid conversion to polycrystalline ice Ih occurs at 150 K. However Dowell and Rinfret [33] contradict this and claim that Ic to Ih conversion would take several hours at 150 K. Dowell and Rinfret [33] give equations for calculating the time taken for the amorphous to Ic conversion and for the Ic to Ih conversion at a given temperature. Their work tends to show some agreement with that of Beaumont et al. [34], with a fast transition being observed for amorphous to Ic and a slower one over a larger temperature range being observed for Ic to Ih. Shallcross and Carpenter [38] were unable to obtain pure ice Ic as it was always contaminated with ice Ih. They found that, in the mixed samples, complete conversion to ice Ih occurred on heating.

However, the situation may not be as simple as Dowell and Rinfret [33] think. Mayer and Pletzer have shown [32] that the transition temperatures depend on the state of the vapor used to make the amorphous ice. They investigated the effects of using baffles and different flow conditions when depositing the amorphous ice and found that different forms of amorphous ice are produced and that this has a dramatic effect on the transition temperatures.

Because of the variations in the transition temperatures and the observed kinetic effects, if one wishes to make samples of polycrystalline ice Ih from water vapor, it is probably best to deposit it directly rather than by annealing ice Ic or amorphous ice. This procedure is discussed below.

Direct Deposition of Hexagonal Polycrystalline Ice Ih

Polycrystalline ice Ih has been deposited directly from water vapor [38–46] at higher temperatures than those used for amorphous ice or Ic ice, and Hobbs [28] has reviewed much of the literature in this area. There seems to be a general agreement of many researchers [38–41, 45] that, above 173 K, polycrystalline ice Ih alone is formed, although the temperature of 173 K varies slightly in some works [42]. In [38, 43, 44, 46], all report polycrystalline ice Ih forming at various temperatures that are all greater than 173 K. Publication [42] appears to be the only one in disagreement with the above observations. In that paper, the authors report that the temperature needs to be above 193 K to form pure hexagonal ice. However, the results reported in that paper are a little suspect. It is possible that some ice deposited at lower temperatures was still present at higher temperatures because the water supply was frozen but not shut off from the chamber while the substrate was cooled. However, there is insufficient detail in the paper to confirm this. In addition, ice Ic was not

observed in that work, which is somewhat surprising. The authors mention early difficulties with the temperature control, and, although they claim that these difficulties were overcome, perhaps the temperature measurements were still subject to some uncertainty. Another work [43] by the same authors also indicates that ice Ih forms at 188 K, and this is inconsistent with their work in [42].

Blackman and Lisgarten [41] have also reported on D_2O and found, in that case, that the temperature needs to be 3 to 4 K higher than 173 K in order to directly deposit hexagonal polycrystalline D_2O ice.

In contrast to the above, an early paper by Vegard and Hillesund [47] indicates that hexagonal ice (Ih) may form at temperatures as low as 88 K with rapid deposition of either H_2O or D_2O vapor. However, the authors admit that there is considerable experimental error in the lattice parameters obtained by X-ray diffraction, so, possibly, the samples actually contained some ice Ic and/or amorphous ice. However, much more recent work [48, 49] has shown that the substrate affects the crystallization kinetics and that vapor deposition of H_2O onto a crystalline ice substrate can produce additional crystalline ice at low temperatures.

The Possibility of Converting Polycrystalline Ice Back to Amorphous Ice

Hobbs states in his review [28] that when polycrystalline ice Ih is formed by vapor deposition, it is never observed to transform to ice Ic even when the temperature is lowered well below 173 K. This statement is supported by a number of other researchers [38, 42, 44, 46]. This result is expected since both amorphous ice and ice Ic are metastable with respect to ice Ih. In spite of this, however, recent work by Kouchi and Kuroda [50] has shown that ice Ic will transform to amorphous ice under the influence of UV light if the temperature is below 70 K. They used a flux of ca. 10^{12} photons cm^{-2} s^{-1} and a wavelength range of 110 to 400 nm. Between 50 and 70 K, it took a half an hour to one hour to perform the transformation. However above 70 K, no transformation was observed even after five hours of exposure to UV light.[4] The authors also refer to other work by Lepault et al. [51] in which ice Ic and Ih was transformed to amorphous ice under the influence of 100 kV electrons. Upon heating, the amorphous ice was converted back to polycrystalline ice. From the above results, it is clear that polycrystalline ice Ih will remain in this form above 70 K if it is not exposed to high energy ionizing radiation. Even below 70 K, it takes considerable exposure to high energy ionizing radiation to alter the morphology of polycrystalline ice Ih.

[4] In the present work, the ice was never cooled below 70 K and was only exposed to UV light for periods of several minutes. There is thus no possibility that the polycrystalline ice could have converted to amorphous ice.

Best Method for Producing Polycrystalline Ice Ih

Because of the wide disagreement about the temperatures and times necessary to anneal amorphous ice and ice Ic to produce ice Ih, it is preferable to produce polycrystalline ice Ih directly from the vapor phase. To do this, it seems that it is necessary to use a substrate temperature greater than 173 K for H_2O and 177 K for D_2O. These temperatures are in agreement with most of the literature in this area.

APPENDIX 2

THE EFFECT ON LIFETIMES OF EXCITED STATES

The lifetime of the excited state will be the reciprocal of the Einstein coefficient for spontaneous emission of light, A, which is given by [52]

$$A = 8\pi hB/\lambda^3, \tag{3}$$

where h is the Planck constant; λ is the wavelength of the emitted radiation; and B is the Einstein coefficient for stimulated emission or absorption, which is given by [52]

$$B = \left|-e\int \phi_f r \phi_i d\tau\right|^2/(6\varepsilon_0\hbar^2). \tag{4}$$

In this expression, e is the electronic charge, r is the position operator, ε_0 is the permittivity of free space, and $\hbar$ is $h/(2\pi)$. The integral represents the overlap of the wavefunction of the initial state, ϕ_i, and the final state, ϕ_f. The only dependence of B on the mass is via these wavefunctions.

There are several ways in which the substitution of one isotope for another can affect the lifetime of an electronic transition. Firstly, the substitution of the heavier isotope for the lighter isotope affects the vibratory motion of the molecule and, hence, affects (by a calculable amount) the electronic excitation energy. The wavelength of the emitted light is thus altered. This wavelength shift can then affect the transition probability and, hence, the lifetime of the luminescence according to Eq. (3).

Consider mechanism 3 proposed by Quickenden et al. [7, 8] for the 420 nm emission from UV-excited ice. If the wavelength shifts by 1.4 nm (the maximum likely shift [6]) when D_2O is substituted for H_2O, then a change in the lifetime of 1.0% would be expected. Such a small change would be undetectable in the present work.

A second and even smaller effect on the lifetime is caused by an isotopic effect on the overlap of the wavefunctions of the upper and lower electronic states. If the above mechanism for the 420 nm luminescence is correct, then Eqs. (3) and (4) predict that the change in the overlap of the wavefunctions of the upper and lower electronic states will have a negligible effect on the lifetime of the luminescence. This is because the wavefunction for a hydrogen atom involves the reduced

mass of the atom, which is obtained by taking the reciprocal of the sum of the reciprocals of the nuclear and electronic masses. For a hydrogen atom, the reduced mass is 9.10×10^{-31} kg, while, for deuterium, it is 9.11×10^{-31} kg. The difference between these masses is only ca. 0.1% so that any effect on the lifetime of an excited state would be negligible, effectively because the electron's mass rather than the mass of the nucleus dominates the wavefunction.

There could also be a third effect of isotopic substitution on an excited state lifetime. This could arise for a diatomic molecule when an electronic transition is involved and the populations of the vibrational sublevels are changed due to the change in energy spacing [53]. However, this change will be the same in the upper and lower electronic states, so the population changes will be the same in both cases and there will be very little change in the vibrational levels that are involved in most of the emission. Also, generally, most of the emission arises from the ground vibrational state and not from the higher ones.

In summary, it is clear that isotopic substitution has a negligible effect on the lifetime of an excited species. Thus, if the mechanism of the 420 nm luminescence in ice involves an electronic transition as the rate-determining step, one would expect to see no significant change in the rate constants for the first-order luminescence rises and decays.

ACKNOWLEDGMENTS

The support from an Australian Research Council Small Grant is gratefully acknowledged. BJS gratefully acknowledges an Australian Postgraduate Award during the course of this work. We would also like to thank Professor R.E. Johnson from the University of Virginia for many useful discussions.

REFERENCES

1. Quickenden, T.I., Litjens, R.A.J., Freeman, C.G., and Trotman, S.M., *Chem. Phys. Lett.*, 1985, vol. 114, no. 2, p. 164.
2. Litjens, R.A.J., *PhD Thesis*, Perth: Univ. of Western Australia, 1986.
3. Litjens, R.A.J. and Quickenden, T.I., *J. Phys. Colloq.*, 1987, p. C1/59.
4. Matich, A.J., *PhD Thesis*, Perth: Univ. of Western Australia, 1992.
5. Lennon, D., Quickenden, T.I., and Freeman, C.G., *Chem. Phys. Lett.*, 1993, vol. 201, nos. 1–4, p. 120.
6. Matich, A.J., Bakker, M.G., Lennon, D., and Quickenden, T.I., *J. Phys. Chem.*, 1993, vol. 97, no. 41, p. 10539.
7. Quickenden, T.I., Green, T.A., and Lennon, D., *J. Phys. Chem.*, 1996, vol. 100, no. 42, p. 16 801.
8. Quickenden, T.I., Hanlon, A.R., and Freeman, C.G., *J. Phys. Chem. A*, 1997, vol. 101, no. 25, p. 4511.
9. Khusnatdov, N.N. and Petrenko, V.F., in *Physics and Chemistry of Ice*, Maeno, N. and Hondoh, T., Eds., Sapporo: Hokkaido Univ. Press, 1992.
10. Langford, V.S., McKinley, A.J., and Quickenden, T.I., *Acc. Chem. Res.*, 2000, vol. 33, no. 10, p. 665.
11. Selby, B.I., *PhD Thesis*, Perth: Univ. of Western Australia, 2002.
12. Buxton, G.V., Gillis, H.A., and Klassen, N.V., *Can. J. Chem.*, 1976, vol. 54, no. 1, p. 367.
13. Maria, H.J. and McGlynn, S.P., *J. Chem. Phys.*, 1970, vol. 52, no. 7, p. 3402.
14. Selby, B.J., Quickenden, T.I., and Freeman, C.G., *Kinet. Catal.*, 2003, vol. 44, no. 1, p. 5.
15. Flournoy, J.M., Baum, L.H., and Siegel, S., *J. Chem. Phys.*, 1962, vol. 36, no. 8, p. 2229.
16. Plonka, A., Kroh, J., Lefik, W., and Bogus, W., *J. Phys. Chem.*, 1979, vol. 83, no. 14, p. 1807.
17. Eckner, U., Helmreich, D., and Engelhardt, H., in *Physics and Chemistry of Ice*, Whalley, E., Jones, S.J., and Gold, L.W., Eds., Ottawa: Royal Society of Canada, 1973.
18. Warman, J.M., de Haas, M.P., and Verberne, J.B., *J. Phys. Chem.*, 1980, vol. 84, no. 10, p. 1240.
19. Siegel, S., Baum, L.H., Skolnik, S., and Flournoy, J.M., *J. Chem. Phys.*, 1960, vol. 32, no. 4, p. 1249.
20. Swiatla-Wojcik, D. and Buxton, G.V., *Phys. Chem. Chem. Phys.*, 2000, vol. 2, no. 22, p. 5113.
21. Livingston, F.E., Smith, J.A., and George, S.M., *J. Phys. Chem. A*, 2002, vol. 106, no. 26, p. 6309.
22. Crowell, R.A. and Bartels, D.M., *J. Phys. Chem.*, 1996, vol. 100, no. 45, p. 17713.
23. Babenko, S.D., Benderskii, V.A., and Krivenko, A.G., *Dokl. Akad. Nauk SSSR*, 1976, vol. 231, no. 4, p. 907.
24. Taub, I.A. and Eiben, K., *J. Chem. Phys.*, 1968, vol. 49, no. 6, p. 2499.
25. Ghormley, J.A. and Hochanadel, C.J., *J. Phys. Chem.*, 1971, vol. 75, no. 1, p. 40.
26. Quickenden, T.I. and Irvin, J.A., *J. Chem. Phys.*, 1980, vol. 72, no. 8, p. 4416.
27. Litjens, R.A.J., Quickenden, T.I., and Freeman, C.G., *Appl. Opt.*, 1999, vol. 38, no. 7, p. 1216.
28. Hobbs, P.V., *Ice Physics*, Oxford: Clarendon, 1974.
29. Freeman, C.G., Quickenden, T.I., Litjens, R.A.J., and Sangster, D.F., *J. Chem. Phys.*, 1984, vol. 81, no. 12, p. 5252.
30. Sivakumar, T.C., Rice, S.A., and Sceats, M.G., *J. Chem. Phys.*, 1978, vol. 69, no. 8, p. 3468.
31. Narten, N.H., Venkatesh, C.G., and Rice, S.A., *J. Chem. Phys.*, 1976, vol. 64, no. 3, p. 1106.
32. Mayer, E. and Pletzer, R., *J. Chem. Phys.*, 1984, vol. 80, no. 6, p. 2939.
33. Dowell, L.G. and Rinfret, A.P., *Nature*, 1960, vol. 188, no. 4757, p. 1144.
34. Beaumont, R.H., Chihara, H., and Morrison, J.A., *J. Chem. Phys.*, 1961, vol. 34, no. 4, p. 1456.
35. Defrain, A. and Linh, N.T., *C. R. Acad. Sci. Paris, Ser. C*, 1966, vol. 263, no. 22, p. 1366.
36. König, H., *Nachr. Acad. Wiss. Goettingen, Math. Phys. Kl.*, 1942, no. 1, p. 6; *Chem. Zentr.*, 1943, vol. 1, p. 2571.

37. König, H., *Z. Kristallogr.*, 1944, vol. 105, p. 279.
38. Shallcross, F.V. and Carpenter, G.B., *J. Chem. Phys.*, 1957, vol. 26, no. 4, p. 782.
39. Kumai, M.J., *Glaciology*, 1968, vol. 7, no. 49, p. 95.
40. Vertsner, V.N. and Zhdanov, G.S., *Sov. Phys. Crystallogr.*, 1966, vol. 10, no. 5, p. 597.
41. Blackman, M. and Lisgarten, N.D., *Proc. R. Soc. A,* 1957, vol. 239, p. 93.
42. Burton, E.F. and Oliver, W.F., *Proc. R. Soc. A*, 1935, vol. 153, p. 166.
43. Burton, E.F. and Oliver, W.F., *Nature*, 1935, vol. 135, p. 505.
44. Honjo, G., Kitamura, N., Shimaoka, K., and Mihama, K., *J. Phys. Soc. Jpn.*, 1956, vol. 11, no. 5, p. 527.
45. Fernandez-Moran, H., *Ann. N. Y. Acad. Sci.*, 1960, vol. 85, p. 689.
46. Brill, V.R. and Tippe, A., *Acta. Crystallogr.*, 1967, vol. 23, no. 3, p. 343.
47. Vegard, S. and Hillesund, S., *Avhandl. Norske Videnskaps-Akad. Oslo: I. Mat–Naturv. Kl.*, 1942, no. 8, p. 24.
48. Dohnalek, Z., Ciolli, R.L., Kimmel, G.A., Stevenson, K.P., Smith, R.S., and Kay, B.D., *J. Chem. Phys.*, 1999, vol. 110, no. 12, p. 5489.
49. Dohnalek, Z., Kimmel, G.A., Ciolli, R.L., Stevenson, K.P., Smith, R.S., and Kay, B.D., *J. Chem. Phys.*, 2000, vol. 112, no. 13, p. 5932.
50. Kouchi, A. and Kuroda, T., *Nature*, 1990, vol. 344, no. 6262, p. 134.
51. Lepault, J., Freeman, R., and Dubochat, J., *J. Microsc.*, 1983, vol. 132, p. RP3.
52. Eisberg, R. and Resnick, R., *Quantum Physics of Atoms, Molecules, Solids, Nuclei, and Particles*, New York: Wiley, 1974.
53. Herzberg, G., *Molecular Spectra and Molecular Structure*, Toronto: Van Nostrand, 1951.
54. Symons, M.C.R., *J. Chem. Soc., Faraday Trans.*, 1982, vol. 78, no. 6, p. 1953.
55. Box, H.C., Budzinski, E.E., Lilga, K.T., and Freund, H.G., *J. Chem. Phys.*, 1970, vol. 53, no. 3, p. 1059.